CNRS
Centre Nationale de la Recherche Scientifique

INFN
Istituto Nazionale di Fisica Nucleare

The VIRGO-1998 Detection Bench Position Sensor (First Step)

(Draft 7 Sept 1996)

V. Sannibale
(*sanni@virgoa1.in2p3.fr*)

Laboratoire d'Annecy-le-Vieux de Physique des Particules
Chemin de Bellevue BP 110, 74941 Annecy-le-Vieux CEDEX, FRANCE

VIR-NOT-LAP-1390-080
Issue: 1
Date : 24 Mar 1997

VIRGO * A joint CNRS-INFN Project
Project Office: INFN-Sezione di Pisa * Via Livornese, 1291-56010 San Piero a Grado, Pisa Italia.
Secretariat: Telephone (39) 50 880 327 or 880 352 * FAX (39) 50 880 350 * e-mail virgo@pisa.infn.it

1 Introduction

In this note is presented the system of automatic positioning of the detection bench for VIRGO-1998, which is necessary to ensure the correct alignment of the mode cleaner with the dark fringe beam .

The position sensors are two quadrant photodiodes placed onto the detection bench, (in vacuum) which give the error signals to send to the rest of the feedback network.

The main characteristics (dynamics range , sensitivity , degree of freedom and decoupling) are briefly discussed also.

2 Position Sensor Sensitivity

The position sensor sensitivity is defined by the mode matching constraints (the more stringent ones) for the mode cleaner [2].

In order to keep the losses below 10^{-3}, the maximum RMS tilt and RMS displacement allowed (see figure 1) between the beam axis and the mode cleaner axis , are

$$\begin{aligned} \langle \delta r_{m.c.} \rangle &\ll 3\%\ w_0 \\ \langle \delta \theta_{m.c.} \rangle &\ll 3\%\ \theta_\infty, \end{aligned} \tag{1}$$

where w_0 and θ_∞ are the waist and the far field divergence of the mode cleaner.

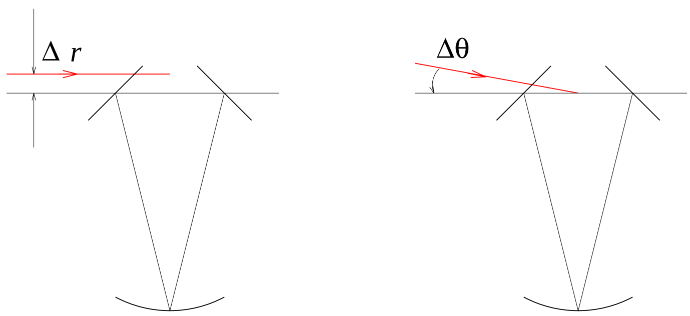

Figure 1: Displacements and tilts for the mode cleaner.

Considering that we have

$$\begin{aligned} w_0 &\simeq 140\ \mu m \\ \theta_\infty &\simeq 2.42 \cdot 10^{-3}\ rad, \end{aligned} \tag{2}$$

we obtain the following maximum displacement and tilt allowed

$$\begin{aligned} \langle \delta r_{m.c.} \rangle &\ll 4.2 \cdot 10^{-5}\ m \\ \langle \delta \theta_{m.c.} \rangle &\ll 7.3 \cdot 10^{-6}\ rad. \end{aligned} \tag{3}$$

To calculate the maximum allowed displacement and tilt for the detection bench, we need to inverse the ABCD matrix that describes the optical path starting from the tower center (supposing that all the bench rotations occur around that axis) and ending to the mode cleaner waist position [3].

The RMS values of the tilt and displacements are given by the following expressions

$$\begin{aligned} \langle \delta r_{d.b} \rangle &= \sqrt{a^2 \langle \delta r^2_{m.c.} \rangle + b^2 \langle \delta \theta^2_{m.c.} \rangle} \\ \langle \delta \theta_{d.b} \rangle &= \sqrt{c^2 \langle \delta r^2_{m.c.} \rangle + d^2 \langle \delta \theta^2_{m.c.} \rangle}. \end{aligned} \tag{4}$$

where a, b, c, d are the elements of the inverse matrix. The numerical values results to be

$$\begin{aligned} \langle \delta r_{d.b.} \rangle &\ll 1.06 \cdot 10^{-4}\ m \\ \langle \delta \theta_{d.b.} \rangle &\ll 2.87 \cdot 10^{-6}\ rad. \end{aligned} \tag{5}$$

3 Principle of Signal Detection

A centered optical system in the paraxial approximation, can be easily described, using the ABCD formalism [1] which relates the displacement and the tilts at the input with those at the output , i.e.

$$\begin{pmatrix} \Delta r_{out} \\ \Delta \theta_{out} \end{pmatrix} = \begin{pmatrix} A & B \\ C & D \end{pmatrix} \begin{pmatrix} \Delta r_{in} \\ \Delta \theta_{in} \end{pmatrix} \qquad \hat{M} = \begin{pmatrix} A & B \\ C & D \end{pmatrix} \tag{6}$$

Using a quadrant photodiode aligned at the end of the optical system, we are able to measure the displacements Δr_{out} from the optical axis.

With two quadrant photodiodes placed at different distances, we have two independent optical systems with $ABCD$ matrix $\hat{M}$ and $\hat{M}'$, whose first lines arranged together gives the following one

$$\left\{ \begin{aligned} \Delta r_{out} &= A \Delta r_{in} + B \Delta \theta_{in} \\ \Delta r'_{out} &= A' \Delta r_{in} + B' \Delta \theta_{in} \end{aligned} \right. , \qquad \hat{T} = \begin{pmatrix} A & B \\ A' & B' \end{pmatrix} \tag{7}$$

This linear system can be inverted, to obtain the displacement and the tilt at the common input[1].

Using this kind of device, we are insensitive to the tilts around the optical axis as well as to the displacements along the same axis.

4 Position Sensor Scheme

For VIRGO-1998 we have decided for the simplest configuration of two quadrant photodiodes Q_1, Q_2 at different distances L_1, L_2 measured starting from the ending mirror of the telescope.

The tilts of the mirrors M_1, M_2, (see figure 2) determines two different focal length on the Oxz and Oyz planes(see figure 3). On consequence, we have two different matrices $\hat{T}_x$ $\hat{T}_y$ for the displacements.

For the Oxz plane, with the following values

$$\begin{aligned} L_1 &= 1.200\ m \quad \text{for} \quad Q_1, \\ L_2 &= 2.634\ m \quad \text{for} \quad Q_2. \end{aligned} \tag{8}$$

we obtain a displacement on Q_2 which is twice than that one on Q_1 if we tilt the bench . For the displacement of the bench, we obtain roughly the same translation on Q_1, Q_2.

In this case, the matrices of the linear system (7) on the Oxz and the Oyz plane will be

[1] Adding on a lens for example (or a set of lenses) to the two optical systems , we can obtain a diagonal matrix for the (7). On the other hand, we increase the complexity of the entire device and in our case, it becomes difficult to reach the needed beam size with the optical paths fitting onto the detection bench.

$$\hat{T}_x = \begin{pmatrix} 0.29495 & 4.7851 \\ 0.29011 & 9.5702 \end{pmatrix}, \qquad \hat{T}_y = \begin{pmatrix} 0.30503 & 4.7799 \\ 0.30985 & 9.5579 \end{pmatrix} \tag{9}$$

The two elements of the first column of each matrix are not exactly equals because of the tilts of the two mirrors (see eqs 6,7 of [3]). The beam sizes at previous distances will be

Spot Size	Q_1 Δx (mm)	Q_2 Δy (mm)
w_x	1.1595	1.4859
w_y	1.1893	1.5342

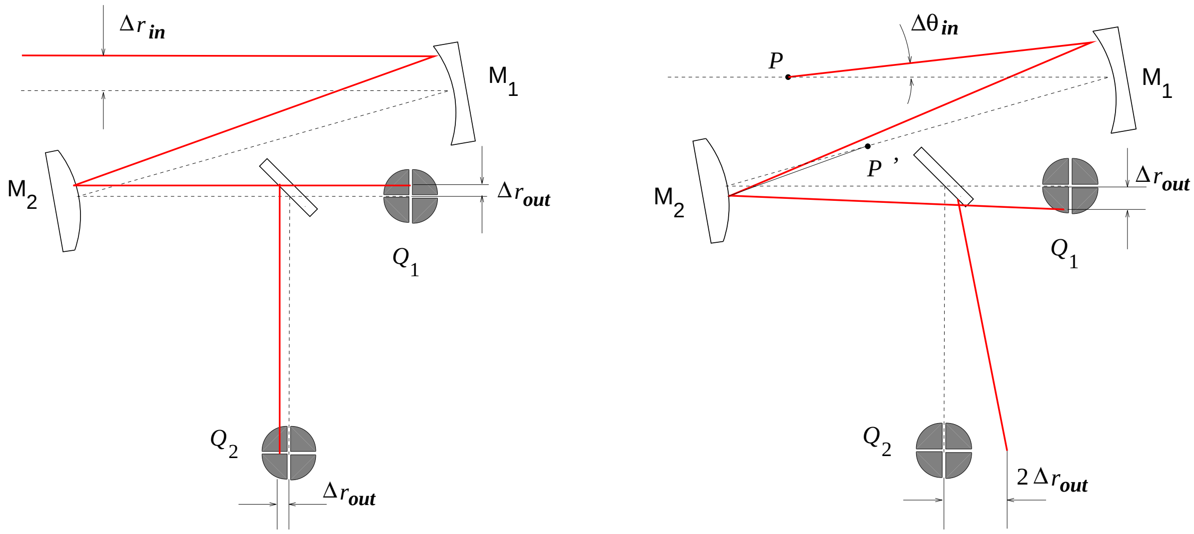

Figure 2: Position Sensor. The left figure is for the displacement case which produces the same displacement for the two quadrant photodiodes Q_1 and Q_2. The right figure is for the tilt around the point P (bench center) which is equivalent to an apparent rotation around the point P'. In this case the displacement on Q_2 is twice the other one on Q_1

5 Quadrant photodiode Sensitivity with Gaussian Beams

The intensity of a Gaussian beam impinging on a quadrant photodiode with a misalignment Δy on the Oy direction is (see fig. 3)

$$|\Psi_{00}(x,y)| = P_{tot}\frac{2}{\pi}\frac{1}{w_x w_y} e^{-2\frac{x^2}{w_x^2} - 2\frac{(y-\Delta y)^2}{w_y^2}} \tag{10}$$

where P_{tot} is the beam power and w_x, w_y the spot sizes of the beam.

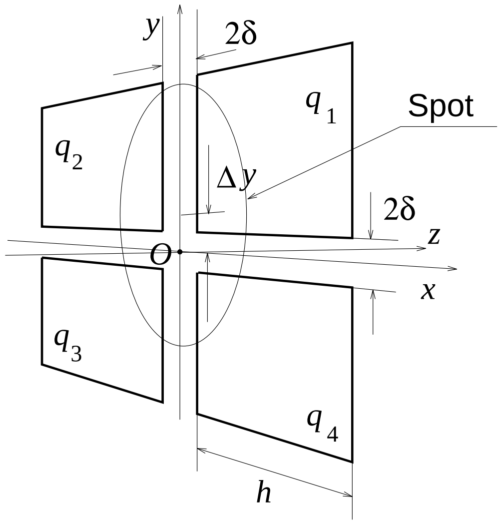

Figure 3: Reference frame for the quadrant photodiode.

Considering a squared quadrant photodiode (for the sake of simplicity), the power arriving to each quadrant , will be given by the following expression

$$
\begin{aligned}
P_1(\Delta y) = \quad P_2(\Delta y) = \quad & F(\delta)\left[\mathrm{erf}\left(\sqrt{2}\frac{h+\delta-\Delta y}{w_y}\right) - \mathrm{erf}\left(\sqrt{2}\frac{\delta-\Delta y}{w_y}\right)\right] \\
P_3(\Delta y) = \quad P_4(\Delta y) = \quad & F(\delta)\left[\mathrm{erf}\left(\sqrt{2}\frac{h+\delta+\Delta y}{w_y}\right) - \mathrm{erf}\left(\sqrt{2}\frac{\delta+\Delta y}{w_y}\right)\right]
\end{aligned} \tag{11}
$$

where

$$F(\delta) = \frac{P_{tot}}{4}\left[\mathrm{erf}\left(\sqrt{2}\frac{h+\delta}{w_x}\right) - \mathrm{erf}\left(\sqrt{2}\frac{\delta}{w_x}\right)\right] \tag{12}$$

$$\mathrm{erf}(\alpha) = \frac{2}{\sqrt{\pi}}\int_0^\alpha d\zeta e^{-\zeta^2} \tag{13}$$

h is the square side of each quadrant and 2δ is the gap between each the elements of the photodiode.

The power ΔP which gives the error signal for the displacements will be

$$\Delta P(\Delta y) = [P_1(\Delta y) + P_2(\Delta y)] - [P_3(\Delta y) + P_4(\Delta y)]\,. \tag{14}$$

In terms of current, we have

$$\Delta i(\Delta y) = \eta \Delta P(\Delta y), \tag{15}$$

where η is the photodiode responsivity.

The displacement Δy on the quadrant photodiodes Q_1 and Q_2, corresponding to the maximum allowed tilt or displacement of the detection bench, are

Detec. Bench Movement	Q_1 Δy (μm)	Q_2 Δy (μm)
displacement	32.3	32.8
tilt	13.7	27.4

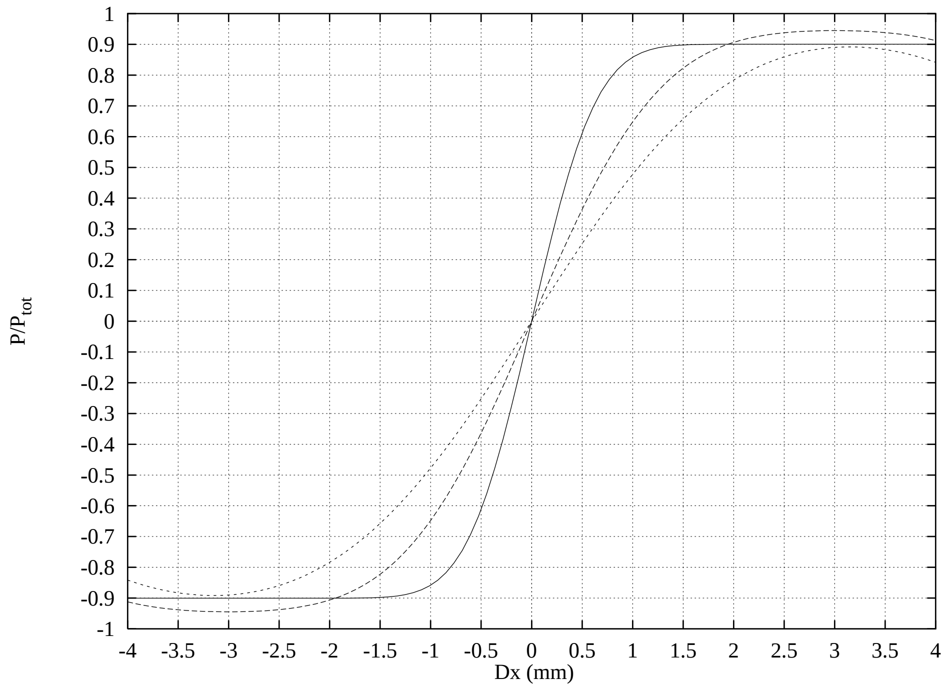

Figure 4: Dynamic range for the quadrant photodiode EG&G YAG-444A-4, using a spot of 1 mm (continuous line), 2 mm (dashed line), 3 mm (dotted line).

Considering the following values for the quadrant photodiode EG&G YAG-444A-4

$$\begin{aligned} 2\delta &= 0.125\ mm & \text{gap} \\ h &= 5.75\ mm & \text{quadrant radius} \\ \eta &= 0.5\frac{A}{W} & \text{nominal responsivity,} \end{aligned} \tag{16}$$

and with

$$P_{tot} = 0.5\ mW, \qquad \text{impinging power} \tag{17}$$

we obtain the following equivalent values of current Δi, for the maximum tilt or displacement at the quadrant photodiodes level

Detec. Bench Movement	Q_1 Δi (μA)	Q_2 Δi (μA)
displacement	8.9	6.5
tilt	3.4	5.44

The tilt does not give a current on Q_1 twice than on Q_2 ,essentially because of the dependency of spot sizes in the (11) and in the (12).

In figure 4 showing the range of a quadrant photodiode for different beam size, we can easily verify that increasing the beam spot size the dynamical range increase and the sensitivity decrease.

In figure 5 is shown the electronic scheme for one quadrant photodiode channel (photoconductive mode).

The parts under vacuum will be the quadrant photodiode, a capacitor and 4 resistors necessary to measure the current flowing through the photodiode. For the vacuum compatibility ($p \simeq 10^{-6}$ $mbar$), it is necessary to use at least the SMD technology for the electronic components.

A low pass filter for the anti-aliasing and a low noise amplifier will be (if necessary) connected before the ADC conversion channel.

The 4 sampled signal will be numerically added and subtracted and then sent to the rest of the feedback network of the position sensor.

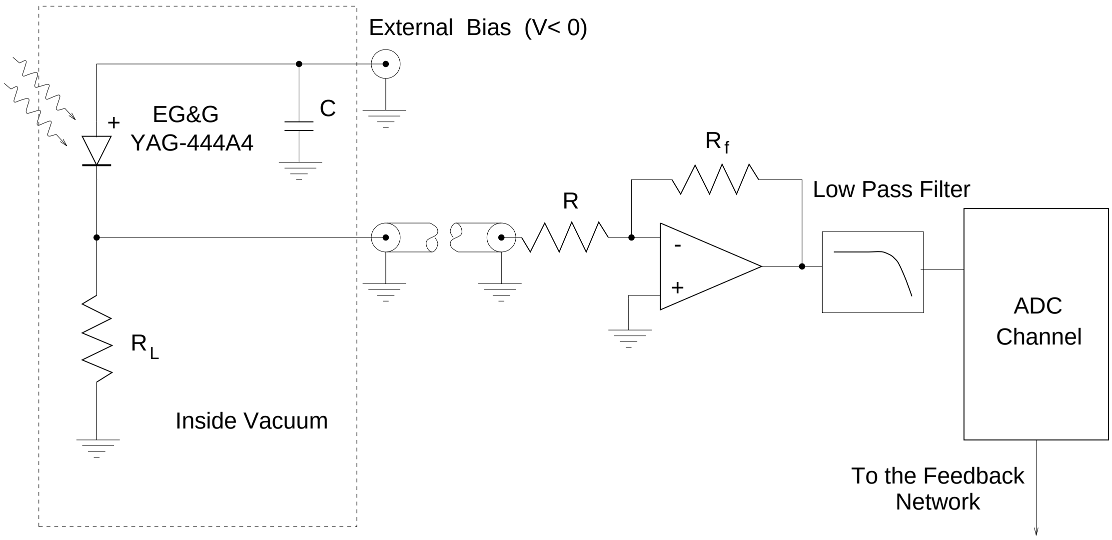

Figure 5: Electronic chain scheme for the voltage sampling of the position sensor. One channel only of the 4 is shown.

References

[1] H. Kogelnik e T. Li, **Laser Beam and Resonators**, *Applied Optics* 23 (1966),3.

[2] A. Dominjon, **Recherche des Ondes Gravitationelles avec l'Interféromètre VIRGO: Étude et Conception de l'Ensemble de Détection du Signal**, *thesis at the L.A.P.P.* (1966).

[3] V. Sannibale, **The VIRGO-1998 Detection Bench Telescope** , *Virgo Note* VIR-NOT-LAP-1390-069 (1996)